

3 1176 00041 6009

CONFIDENTIAL

Copy
RM L57J25

NACA RM L57J25

UNCLASSIFIED

C2

NACA

RESEARCH MEMORANDUM

EXPERIMENTAL HINGE MOMENTS ON TWO FREELY OSCILLATING
TRAILING-EDGE CONTROLS HINGED AT

55 PERCENT CONTROL CHORD

By C. William Martz

Langley Aeronautical Laboratory
Langley Field, Va.

LIBRARY COPY

DEC 27 1957

LANGLEY AERONAUTICAL LABORATORY
LIBRARY, NACA
LANGLEY FIELD, VIRGINIA

CLASSIFICATION CHANGED

Authority of *SP4 #17* *1/18/58*
55A

CLASSIFIED DOCUMENT

This material contains information affecting the National Defense of the United States within the meaning of the espionage laws, Title 18, U.S.C., Secs. 793 and 794, the transmission or revelation of which in any manner to an unauthorized person is prohibited by law.

NATIONAL ADVISORY COMMITTEE FOR AERONAUTICS

WASHINGTON

December 27, 1957

CONFIDENTIAL

UNCLASSIFIED

NATIONAL ADVISORY COMMITTEE FOR AERONAUTICS

RESEARCH MEMORANDUM

EXPERIMENTAL HINGE-MOMENTS ON TWO FREELY OSCILLATING
TRAILING-EDGE CONTROLS HINGED AT
55 PERCENT CONTROL CHORD

By C. William Martz

SUMMARY

Oscillatory hinge-moment characteristics have been obtained from free-flight tests of two rocket-powered models. Each model was equipped with a 60° delta wing featuring a constant-chord, full-span, trailing-edge control hinged at 55 percent control chord. One control was modified by cutting a row of chordwise slots near the leading edge. Data were obtained at near zero angle of attack at Mach numbers from 0.5 to 1.8. Corresponding control reduced frequencies ranged from 0.12 to 0.04.

Results indicate that the hinge-line location of 55 percent control chord did not prevent unstable control aerodynamic damping. Aerodynamic control damping appeared to be more stabilizing as the amplitude of oscillation was increased.

Control restoring moments were stable except for Mach numbers less than about 0.85. The hinge-line location of 55 percent control chord considerably reduced the relatively high restoring moments of the plain-flap-type control.

The effect of the slots near the leading edge of one control was to decrease the supersonic control restoring moments about 25 percent and to decrease the magnitude of the aerodynamic control damping moments especially at transonic speeds.

INTRODUCTION

Control "buzz" has been a problem ever since airplanes have flown at transonic speeds. Although this single degree-of-freedom flutter of the control about its hinge axis is predicted by potential flow theory (ref. 1), there is experimental indication that shock-separated flow also

may be a significant factor (refs. 1 and 3). Some of the more recent NACA investigations of this problem can be found in references 4 to 8.

Suggested ways of eliminating control buzz usually include the following: the addition of external damping to the control system, stiffening the control system to increase the control natural frequency, and aerodynamic modifications. The last of these methods was attempted in the present investigation.

It was noticed that the supersonic wing theory of reference 1 predicts only stable damping moments for a surface with a pivot axis far enough rearward of its leading edge. Thus, it appeared that theoretical justification existed for attempting to eliminate buzz by the use of a rearward hinge line if an assumption that the control would not be affected by the presence of the wing were accepted. For the controls of the present investigation, the axis location predicted for neutral aerodynamic stability was about 54.5 percent chord.

Therefore, an investigation using a rocket-powered model and employing the free oscillation technique was conducted to measure the oscillatory hinge moments at near zero angle of attack of two trailing-edge controls hinged at 55 percent control chord and installed on a 60° delta wing. One control was modified by cutting a row of chordwise slots near the leading edge to insure stable aerodynamic control restoring moments. Mach numbers ranged from 0.5 to 1.9 and Reynolds number per foot varied from 2×10^6 to 13×10^6 . Data were obtained at control reduced frequencies of 0.12 to 0.04 and at control oscillation amplitudes up to $\pm 5^\circ$.

Results are presented herein and compared with potential flow theory where available.

Some preliminary results of one of the present test flights have been presented previously in reference 7.

SYMBOLS

c	control chord, ft
V	free-stream velocity, ft/sec
M	Mach number
q	free-stream dynamic pressure, lb/sq ft

R	Reynolds number based on a length of 1 foot
M_{δ}	aerodynamic control hinge moment per unit deflection, ft-lb/radian
C_h	control hinge-moment coefficient, $\frac{\text{Control hinge moment}}{2M'q}$
δ	control surface deflection, positive trailing edge down, radians except as noted
$\dot{\delta}$	time derivative of control surface deflection, radians/sec
$\Delta\delta$	amplitude of control oscillation envelope, deg
$C_{h_{\delta},\omega}$	aerodynamic control restoring-moment coefficient, $\frac{\text{Real part of } M_{\delta}}{2M'q}$, per radian
$C_{h_{\dot{\delta},\omega}$	aerodynamic control damping-moment coefficient, $\frac{\text{Imaginary part of } M_{\delta}}{2M'qk}$, per radian
ξ	ratio of actual damping to critical damping
ω	control damped natural frequency, radians/sec
ω_0	control damped natural frequency in still air, radians/sec
k	control reduced frequency, $\omega c/2V$
M'	moment of control area rearward of and about hinge line, ft ³
a_z	model longitudinal acceleration, ft/sec ²

In stability notation the symbols $C_{h_{\delta},\omega}$ and $C_{h_{\dot{\delta},\omega}$ are defined as follows:

$$C_{h_{\delta},\omega} = \frac{\partial C_h}{\partial \delta}$$

$$C_{h_{\dot{\delta},\omega} = \frac{\partial C_h}{\frac{\partial \delta c}{2V}}$$

MODELS AND TESTS

Models

The models used in this investigation consisted of a pointed cylindrical fuselage equipped with 60° clipped-delta wings. Vertical tail fins provided yaw stability. The models were identical except for the control surface. The fuselage consisted of a fabricated aluminum-alloy core wrapped with mahogany. The nose cone was plastic and the tail section was a magnesium tube. A dimensioned sketch of the models is shown in figure 1 and photographs of the model, the control, and a motor-driven cam for exciting the control are shown in figures 2 and 3. A schematic of a similar plucking mechanism is shown in figure 3(b) of reference 6.

The wings were of solid magnesium alloy and had an NACA 65A005 airfoil section. One wing panel embodied a constant-chord (13-percent exposed wing-root chord), full-span, trailing-edge control. The control was hinged at its 55 percent chord and was supported by two bearings. The inboard bearing, located inside the fuselage, was a self-aligning ball bearing and the outboard bearing was a journal bearing.

The controls were made of steel and had a modified double wedge section with a blunt trailing edge. See figure 1 for control section. The gap between the wing and the control was 0.07 inch for model A and 0.06 inch for model B. The control of model B differed from the control of model A in that a row of slots was cut near the leading edge as shown in figures 1 and 2. The total slot area was 16.5 percent of the control area.

Experimentally determined dynamical constants of both models are presented in table I.

Preflight Tests

Preflight tests were conducted to determine the structural or tare damping of the control system as well as to obtain the spring constant and inertia of the control system. It was found that the tare damping of the system remained fairly constant under no load after the bearings were cleaned and lubricated with Molykote (a commercial preparation similar in appearance to graphite). Considerable effort was expended to evaluate the effect of external control loads on the tare damping. However, this effect was obscured by friction between the loading apparatus and the control surface at the point of load application.

Since it was anticipated that the controls would oscillate during flight at frequencies less than the still-air value, an attempt was made

to determine what effect oscillation frequency would have on the tare damping. This was done by clamping weights near the trailing edge of the control surface so as to increase the inertia of the system and thereby lower the natural frequency. Tare damping records for three additional frequencies (down to about 20 cps) were obtained for both models. Results of these tests are presented in the section entitled "Results and Discussion."

Flight Tests

The flight tests were conducted at the Langley Pilotless Aircraft Research Station at Wallops Island, Va. Both models were boosted to a Mach number of about 1.9 and coasted back down the Mach number range. It was during this coasting period that the data were obtained. Longitudinal deceleration varied from 1/2 to 7 times the acceleration of gravity.

Existing flight conditions resulted in the values of Reynolds number and dynamic pressure presented in figures 4 and 5 as a function of Mach number.

INSTRUMENTATION

Inductance-type instruments measured time histories of control deflection, total pressure, and normal acceleration of both wing panels. These data were telemetered to a ground receiving station and recorded. Response of the measuring and recording instrumentation was such as to require only a small correction to the recorded data at the frequencies encountered in the tests.

A radiosonde was used to obtain atmospheric data at all flight altitudes. Flight-path data were obtained from SCR-584 tracking radar, and CW Doppler radar was used to determine flight velocity and longitudinal acceleration.

TECHNIQUE

The free-oscillation technique was used in this investigation. The controls were plucked periodically by means of a motor-driven cam (see fig. 3 for photographs of the control plucking system) and the resultant free oscillations of the control were recorded as shown in figure 6. With the assumptions that the control motion was effectively restricted to one degree of freedom and that the aerodynamic damping forces on the

control could be represented adequately by viscous forces, the in-phase or restoring component of the control hinge moments was obtained from the frequency of the control oscillations and the control out-of-phase or damping component was determined from the rate of logarithmic growth or decay of the oscillation. The procedure used in reducing the data to obtain the aerodynamic hinge-moment coefficients is presented in the appendix.

The frequency of the plucking action was 3 cycles per second for both models. The amplitude at which the controls of models A and B were released at the end of their respective plucking actions was 2.75° and 7° .

ACCURACY

It is estimated that errors in the basic quantities are about as follows:

Quantity	Error
M	± 0.01
V	± 10
q	± 50
δ , deg	± 0.4
$\Delta\delta$, deg	± 0.2
ξ_0 , percent	± 5 to ± 10
ξ , percent	± 5 to ± 10
ω , percent	± 1

RESULTS AND DISCUSSION

Control Tare Damping

Control structural or tare damping values are presented in figure 7 as a function of deflection amplitude. The data labeled "original calibration" were measured by the Langley Instrument Research Division about two weeks before the flight tests were conducted. The data for the curves labeled "on launcher" were obtained seconds before the flight tests. These values were later found to be somewhat greater than those of the original calibration. Since the on launcher values were recorded at the time of the flight test, they were used in the reduction of the aerodynamic control damping data.

As previously mentioned, the effect of frequency on tare damping was investigated for both controls at frequencies ranging from the control

still-air frequency (see table I) to about 20 cycles per second through direct damping measurements. Results of these measurements indicated that the tare damping of the control systems was not viscous or hysteretic, but correlated best to the premise that percent critical damping is independent of frequency of oscillation. This result was used in the reduction of the flight data as shown in the appendix.

Control Aerodynamic Damping

Measured variations of control damping moment coefficient with Mach number are presented in figure 8 to indicate (in coefficient form) the relative amounts of tare damping and aerodynamic damping which comprise the total control damping. Both sets of tare damping data are included to show the effect of their differences on the aerodynamic damping results. As can be seen, the aerodynamic damping is a small part of the total control damping at low subsonic speeds and at the higher supersonic speeds. It is in these ranges that moderate differences in tare damping correspond to large percentage changes in aerodynamic damping.

Figure 8 shows that the total damping of the control system was stable throughout the Mach number range for the oscillation amplitudes presented. This plot also indicates that the location of the hinge axis at 55 percent control chord did not prevent the occurrence of unstable aerodynamic control damping. However, the instabilities were mild and resulted in constant amplitude oscillations only slightly greater than the initial input amplitude.

The effect of oscillation amplitude is shown in figure 9 in which the aerodynamic control damping moment coefficient $C_{h\delta, \omega}$ is presented as a function of Mach number for various deflections. The on launcher tare damping values were used in obtaining these results. The data show that the aerodynamic control damping was more stable at the larger amplitudes of oscillation. However, it should be pointed out that this effect was not large and could have been distorted considerably by inaccuracies in tare damping values. Shown for comparison in figure 9(a) are theoretical values of $C_{h\delta, \omega}$ extracted from reference 1. These values were computed for the measured values of reduced-frequency parameter which are presented in figure 10 as a function of Mach number for both models.

The fact that the small amplitude data at the lowest Mach numbers indicate unstable aerodynamic damping is believed to be an indication of incorrect values of tare damping. As previously pointed out, the aerodynamic damping is very sensitive to changes in tare damping at these low Mach numbers. For the same reason, it is felt that the higher supersonic data indicate only that the aerodynamic damping is very close to zero and becomes more stable with increasing Mach number.

Concerning the effects of the slots in one control, it appears that the absolute magnitude of aerodynamic damping is decreased by the slots especially at transonic speeds. There is no significant difference in the general level of aerodynamic damping for the slotted control.

Control Restoring Moments

The aerodynamic in-phase or restoring moment coefficient $C_{h\delta, \omega}$ is presented in figure 11 as a function of Mach number for both controls investigated. These data were measured at the deflection ranges indicated. It should be mentioned that frequency was found to have no systematic variation with amplitude of oscillation for the model B control as measured at several Mach numbers and remained within about $\pm 1\frac{1}{2}$ cycles per second of its mean value for amplitudes up to $\pm 6^\circ$.

Shown in figure 11 for comparison are theoretical values computed from the potential flow results of reference 1 which do not consider the presence of the wing or the control cut-out for the bearing support.

The experimental results of both controls indicate stable restoring moments except for Mach numbers less than about 0.85. Although this was not expected, it is reasonable to attribute this stability to the control cut-out which apparently had a powerful load relieving effect on the control area forward of the hinge line.

It might be pointed out that the hinge-line location at 55 percent chord effectively reduces the relatively high hinge moments of the plain flap-type control (leading-edge hinge line). Values of $C_{h\delta, \omega}$ for the plain flap, if based on the same moment area as the present test results (that rearward of 55 percent control chord), would vary from about -5 to -12 (ref. 4).

Comparison of the slotted-control data with the solid-control data indicates that the effect of the slots was to reduce the absolute magnitude of $C_{h\delta, \omega}$. Thus, it appears that the slots acted to spoil the lift on the control rearward of the hinge line as well as forward of the hinge line. The reduction in restoring moment varied from 20 to 30 percent at supersonic speeds.

Other Remarks

Comparison of the hinge-moment results of the present test with the theory of reference 1 is poor. The primary reason for this result is believed to be the load relieving effect of the control bearing support

cut-outs. The fact that the controls acted as though their hinge lines were forward of 50 percent control mean aerodynamic chord is indicated by the stable restoring moments. This suggests that the effective hinge-line location with respect to damping moments also was forward of the actual location. Thus, it appears that an actual hinge-line location rearward of 55 percent control chord (to counteract the effect of the cutout) would have been a better choice to prevent unstable aerodynamic damping. More specifically, the possibility of "buzz" prevention by means of a rearward hinge line location still exists.

CONCLUDING REMARKS

The use of a hinge-line location of 55 percent control chord did not prevent the occurrence of unstable control aerodynamic damping. However, the instability was mild and resulted in limited amplitude oscillations only slightly greater than the initial amplitude.

Aerodynamic control damping appeared to be more stabilizing at the larger oscillation amplitudes for all Mach numbers and control amplitudes tested.

Control restoring moments were stable except for Mach numbers less than about 0.85. The hinge-line location at 55 percent chord considerably reduced the relatively high restoring moments of the plain flap-type control.

The effect of the slots near the leading edge of one control was to decrease the supersonic control restoring moments about 25 percent and to decrease the absolute magnitude of the aerodynamic damping moments especially at transonic speeds.

Langley Aeronautical Laboratory,
National Advisory Committee for Aeronautics,
Langley Field, Va., September 30, 1957.

APPENDIX

METHOD OF DATA REDUCTION

The general solution to the single-degree-of-freedom moment equation ($I\ddot{\delta} + D\dot{\delta} + K\delta = 0$) governing the free motion of the control about its hinge axis is the damped sinusoid

$$\delta = A_1 e^{\frac{-Dt}{2I}} \sin(\omega t + \phi)$$

where

- I control mass inertia about the hinge line, $\frac{K_o}{\omega_o^2}$, slug-ft²
- D torsional damping constant of the system, $\frac{\text{ft-lb}}{\text{radians/sec}}$
- K torsional spring constant of the system, ft-lb/radian
- A_1, ϕ constants dependent upon initial conditions and unimportant to this investigation
- t time, sec
- ω the control oscillation frequency, $\sqrt{\frac{K}{I} - \left(\frac{D}{2I}\right)^2}$, radians/sec
- $\frac{D}{2I}$ the logarithmic damping factor, $\frac{d(\log_e A)}{dt}$, per sec
- A amplitude of control oscillation envelope

A dot over a symbol indicates a first-order time derivative and two dots indicate a second-order time derivative.

Subscripts o refer to preflight values measured in still air.

By measuring the frequency and logarithmic damping factor of the control oscillation, values of D and K can be calculated knowing the control system inertia. These values include both structural and aerodynamic terms. The following relationships were used to extract the aerodynamic coefficients:

For the in-phase or restoring-moment coefficient,

$$\left(\begin{array}{c} \text{Aerodynamic} \\ \text{restoring} \\ \text{moment} \end{array} \right) = \left(\begin{array}{c} \text{Total} \\ \text{restoring} \\ \text{moment} \end{array} \right) - \left(\begin{array}{c} \text{Structural} \\ \text{restoring} \\ \text{moment} \end{array} \right) - \left(\begin{array}{c} \text{Accelerational} \\ \text{restoring} \\ \text{moment} \end{array} \right)$$

or

$$-C_{h\delta, \omega} 2M'q\delta = I \left[\omega^2 + \left(\frac{D}{2I} \right)^2 \right] \delta - K_0\delta - a_1 U \sin \delta$$

where U is the control mass unbalance about the hinge line and a_1 is the model longitudinal acceleration. Since the effect of damping on the total restoring moment was negligible for the small values of damping obtained and because the control mass unbalance was quite small, the final working form became

$$C_{h\delta, \omega} = - \frac{I\omega^2 - K_0}{2M'q}$$

These values of $C_{h\delta, \omega}$ should be considered average or effective because of possible aerodynamic nonlinearities.

For the out-of-phase or damping moment coefficient,

$$\left(\begin{array}{c} \text{Aerodynamic} \\ \text{damping} \\ \text{moment} \end{array} \right) = \left(\begin{array}{c} \text{Total} \\ \text{damping} \\ \text{moment} \end{array} \right) - \left(\begin{array}{c} \text{Structural} \\ \text{damping} \\ \text{moment} \end{array} \right)$$

or

$$-C_{h\dot{\delta}, \omega} \left(\frac{c}{2V} \right) (2M'q)\dot{\delta} = D\dot{\delta} - D_0 \frac{\omega}{\omega_0} \dot{\delta}$$

The modifying factor $\frac{\omega}{\omega_0}$ is used in the last term to account for the change in frequency between the preflight still-air measurements of structural damping and the flight measurements of total damping. Its use resulted from measurements which indicated that the structural damping was neither viscous nor hysteretic but such that percent critical damping was independent of frequency. In final form,

$$C_{h\dot{\delta}, \omega} = - \frac{D - D_0 \frac{\omega}{\omega_0}}{\frac{c}{2V} 2M'q}$$

or, since $D = 2I\omega\xi$

$$C_{h\dot{\xi},\omega} = -\frac{2I\omega}{\frac{c}{2V} 2M'q} (\xi - \xi_0)$$

per radian, where the subscript o again refers to preflight still-air values.

REFERENCES

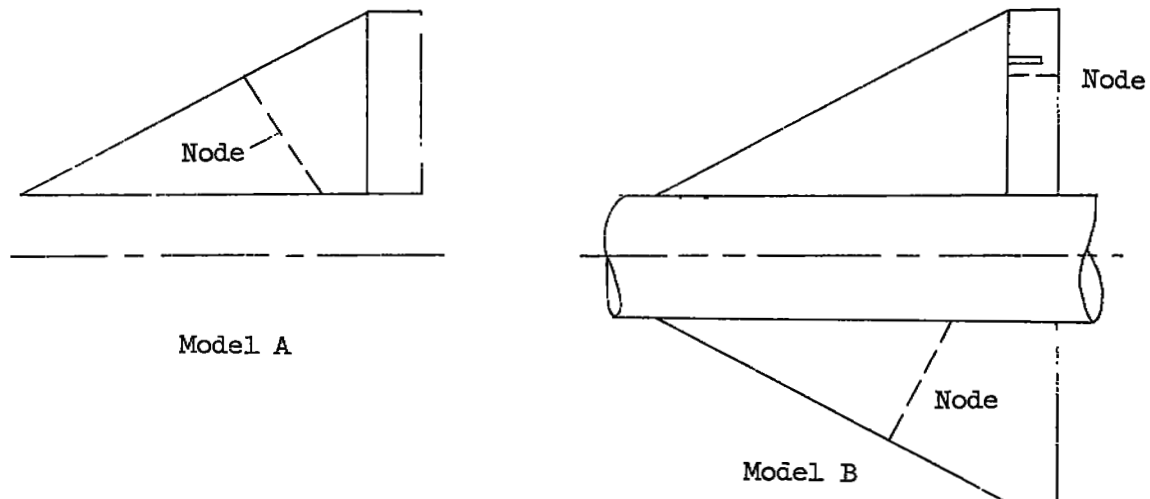
1. Nelson, Herbert C., Rainey, Ruby A., and Watkins, Charles E.: Lift and Moment Coefficients Expanded to the Seventh Power of Frequency for Oscillating Rectangular Wings in Supersonic Flow and Applied to a Specific Flutter Problem. NACA TN 3076, 1954.
2. Erickson, Albert L., and Stephenson, Jack D.: A Suggested Method of Analyzing for Transonic Flutter of Control Surfaces Based on Available Experimental Evidence. NACA RM A7F30, 1947.
3. Henning, Allen B.: Results of a Rocket-Model Investigation of Control-Surface Buzz and Flutter on a 4-Percent-Thick Unswept Wing and on 6-, 9-, and 12-Percent-Thick Swept Wings at Transonic Speeds. NACA RM L53I29, 1953.
4. Reese, David E., Jr., and Carlson, William C. A.: An Experimental Investigation of the Hinge-Moment Characteristics of a Constant-Chord Control Surface Oscillating at High Frequency. NACA RM A55J24, 1955.
5. Tuovila, W. J., and Hess, Robert W.: Aerodynamic Damping at Mach Numbers of 1.3 and 1.6 of a Control Surface on a Two-Dimensional Wing by the Free-Oscillation Method. NACA RM L56A26a, 1956.
6. Martz, C. William: Experimental Hinge Moments on Freely Oscillating Flap-Type Control Surfaces. NACA RM L56G20, 1956.
7. Thompson, Robert F., and Clevenson, Sherman A.: Aerodynamics of Oscillating Control Surfaces at Transonic Speeds. NACA RM L57D22b, 1957.
8. Thompson, Robert F., and Moseley, William C., Jr.: Effect of Hinge-Line Position on the Oscillating Hinge Moments and Flutter Characteristics of a Flap-Type Control at Transonic Speeds. NACA RM L57C11, 1957.

TABLE I

Dynamic Constants of Models

	Model A	Model B
Wing first bending (control wing), cps	---	225
Wing first bending (no-control wing), cps	226	227
Control-wing mode, cps	162	278

See following sketch:



Control still-air frequency, cps	76.1	91.1
--	------	------

No other wing or control modes were apparent from the shake tests up to a frequency of 350 cps.

Control inertia about hinge line, slug-ft ²	0.0002455	0.0001698
Control mass unbalance (tail heavy), slug-ft	0.000343	0.000808

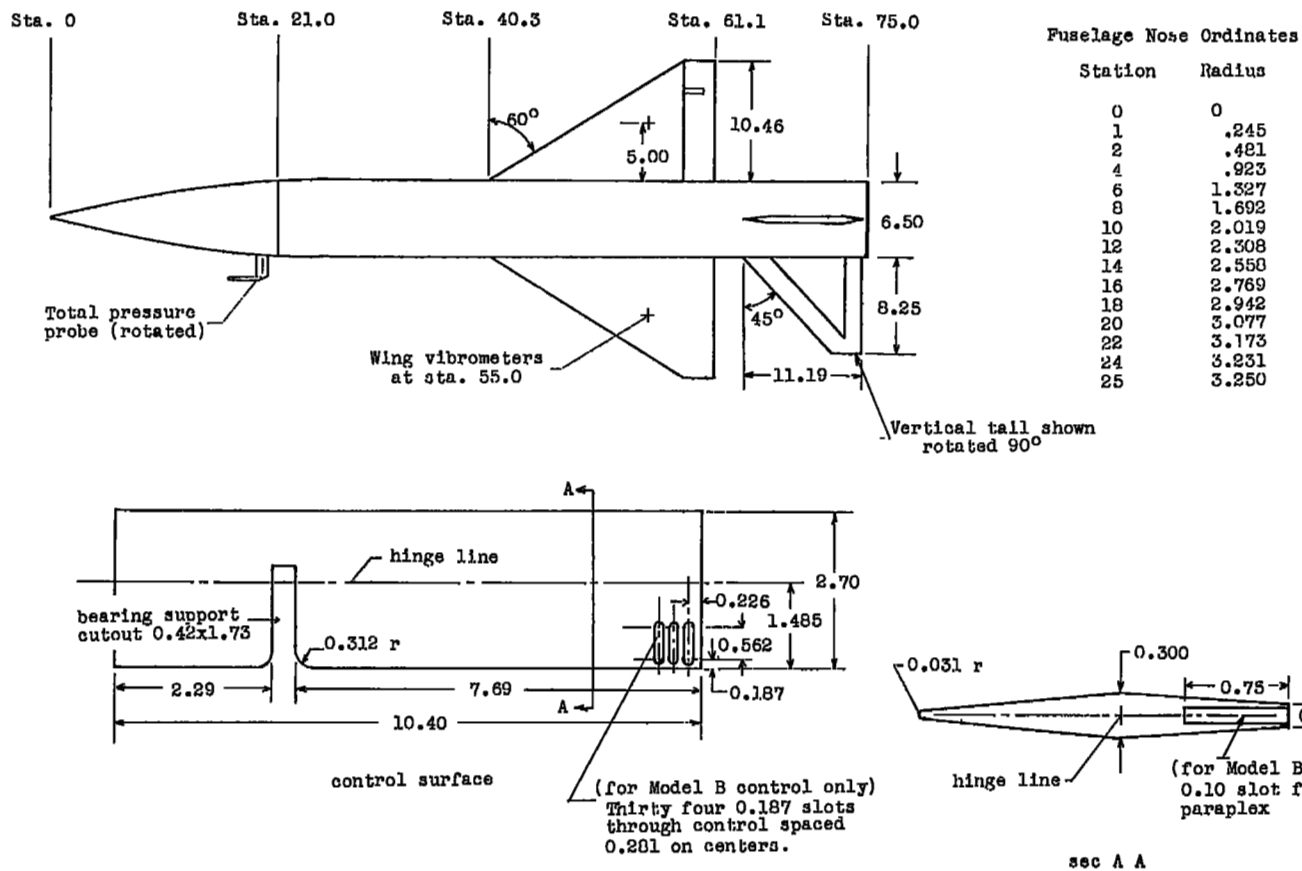
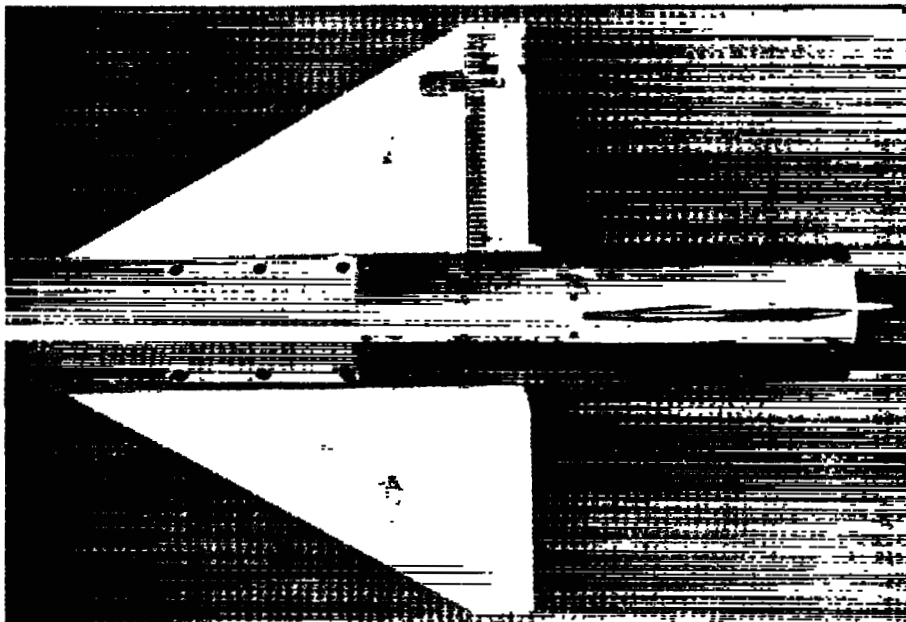


Figure 1.- Details of control damping model. All dimensions are in inches.

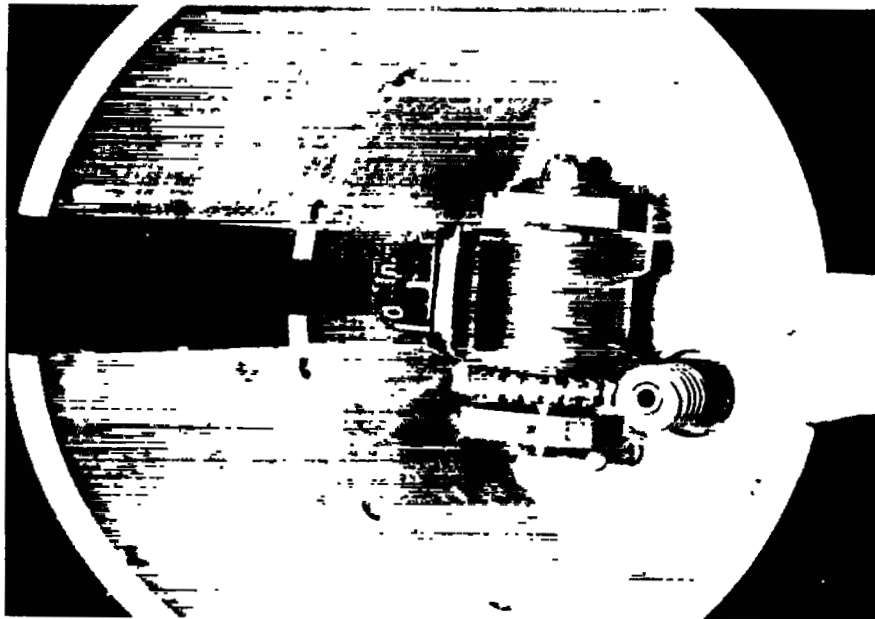


(a) Model A plan view.

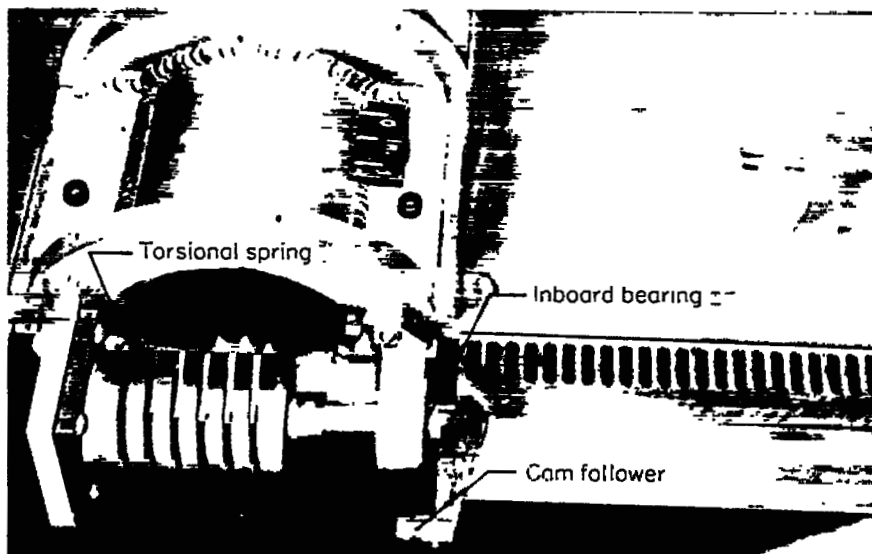


(b) Wing-control close-up; model B. L-57-2775

Figure 2.- Model photographs.



(a) Rotating cam.



(b) Cam follower and control system. L-57-2776

Figure 3.- Photographs of model plucking system.

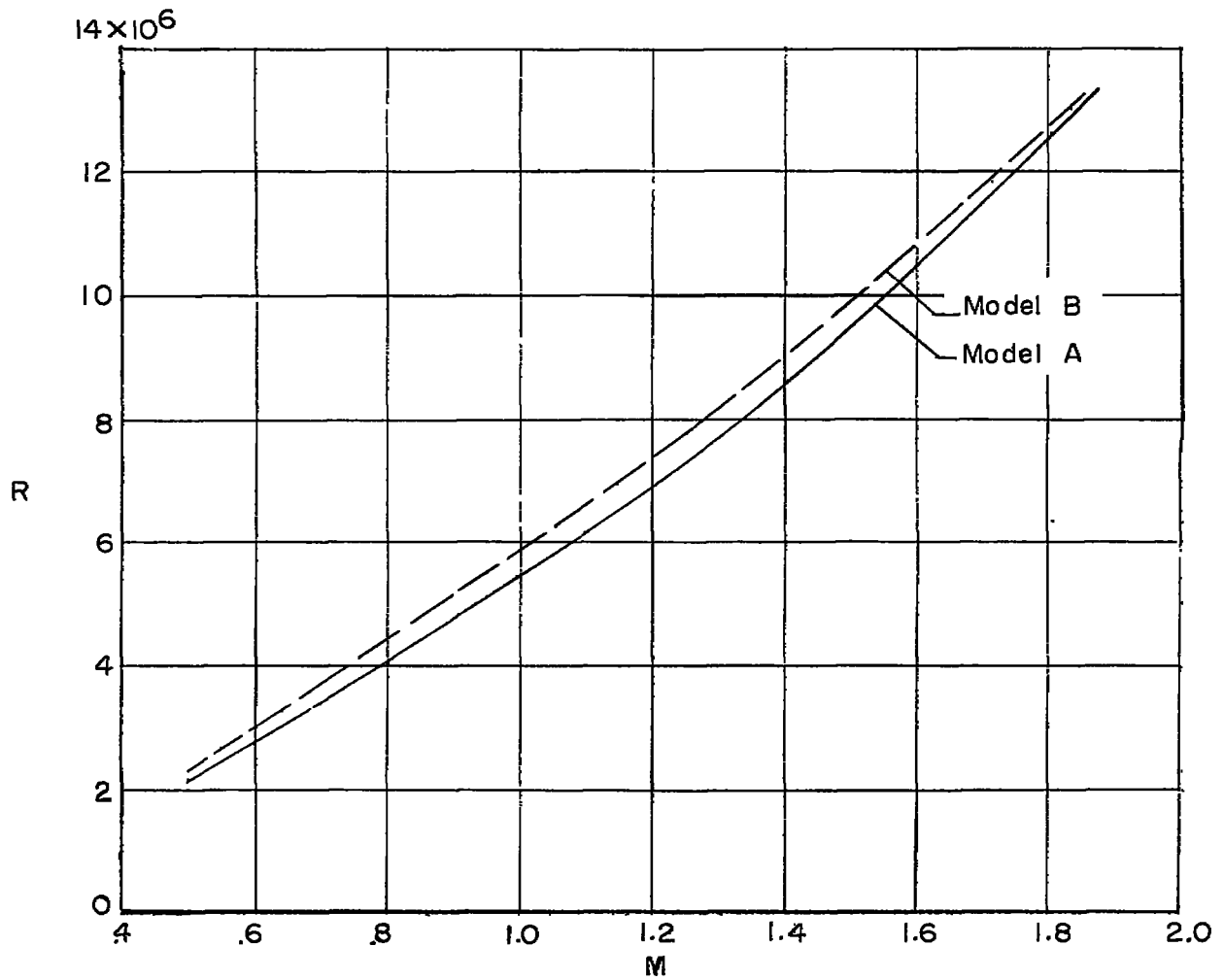


Figure 4.- Variation of Reynolds number with Mach number.

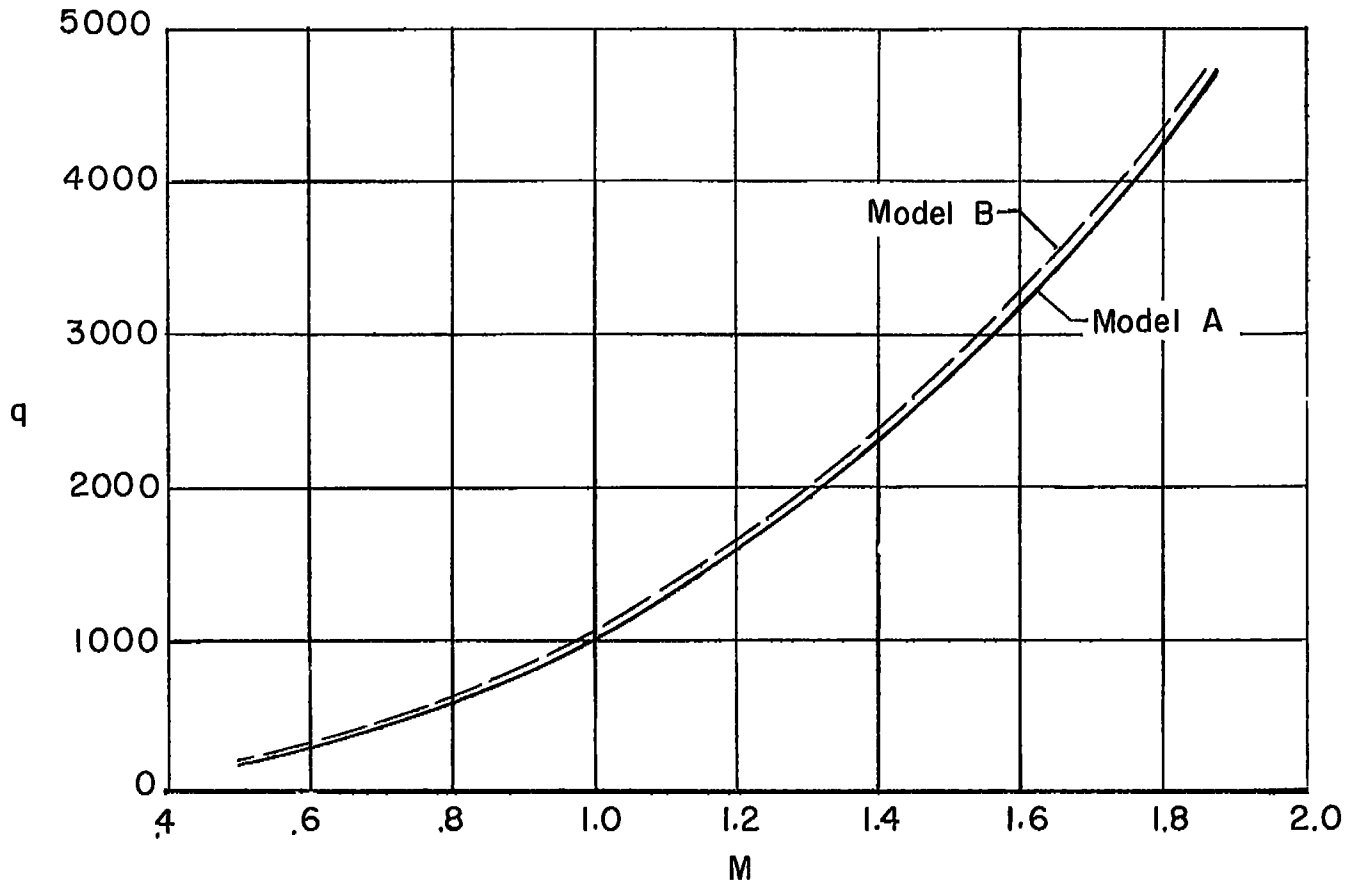
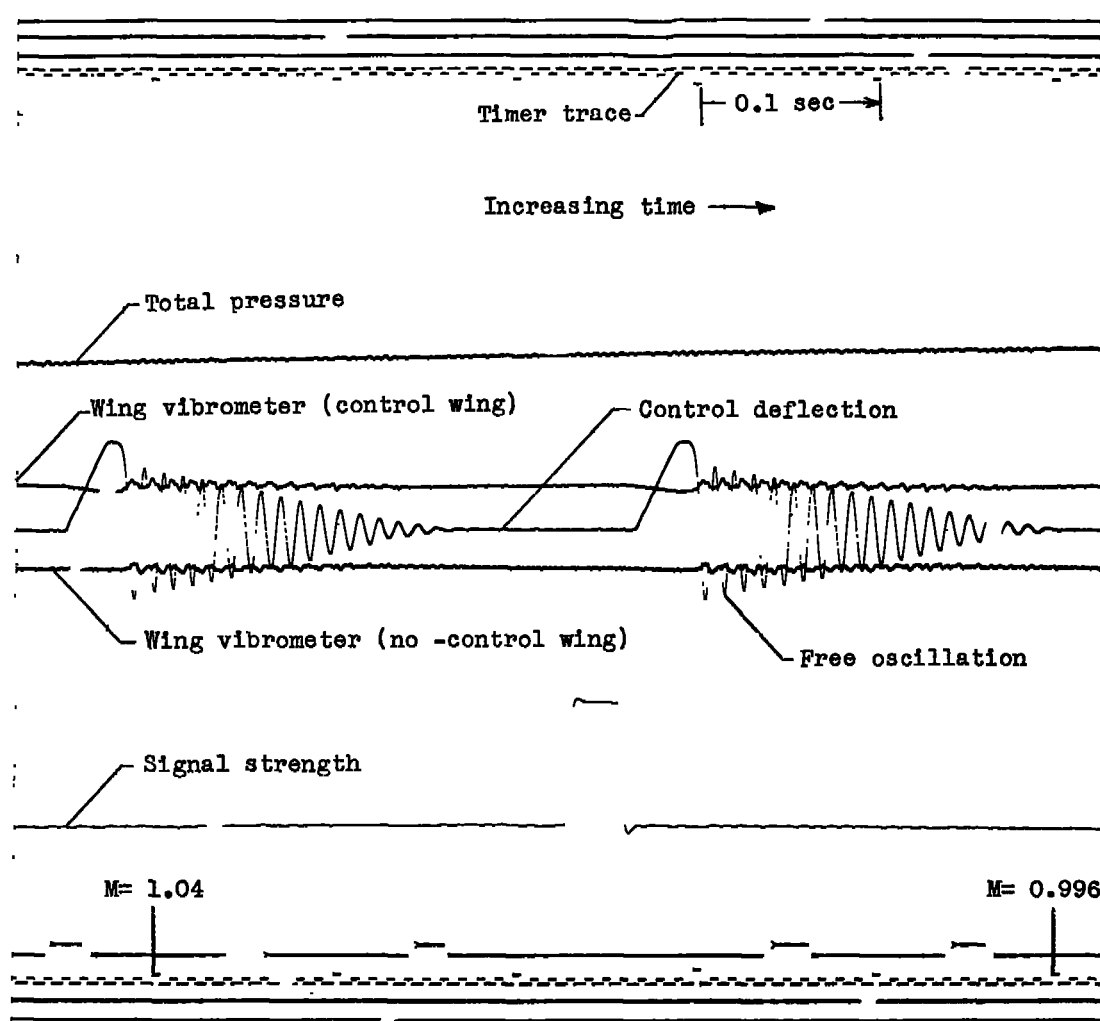
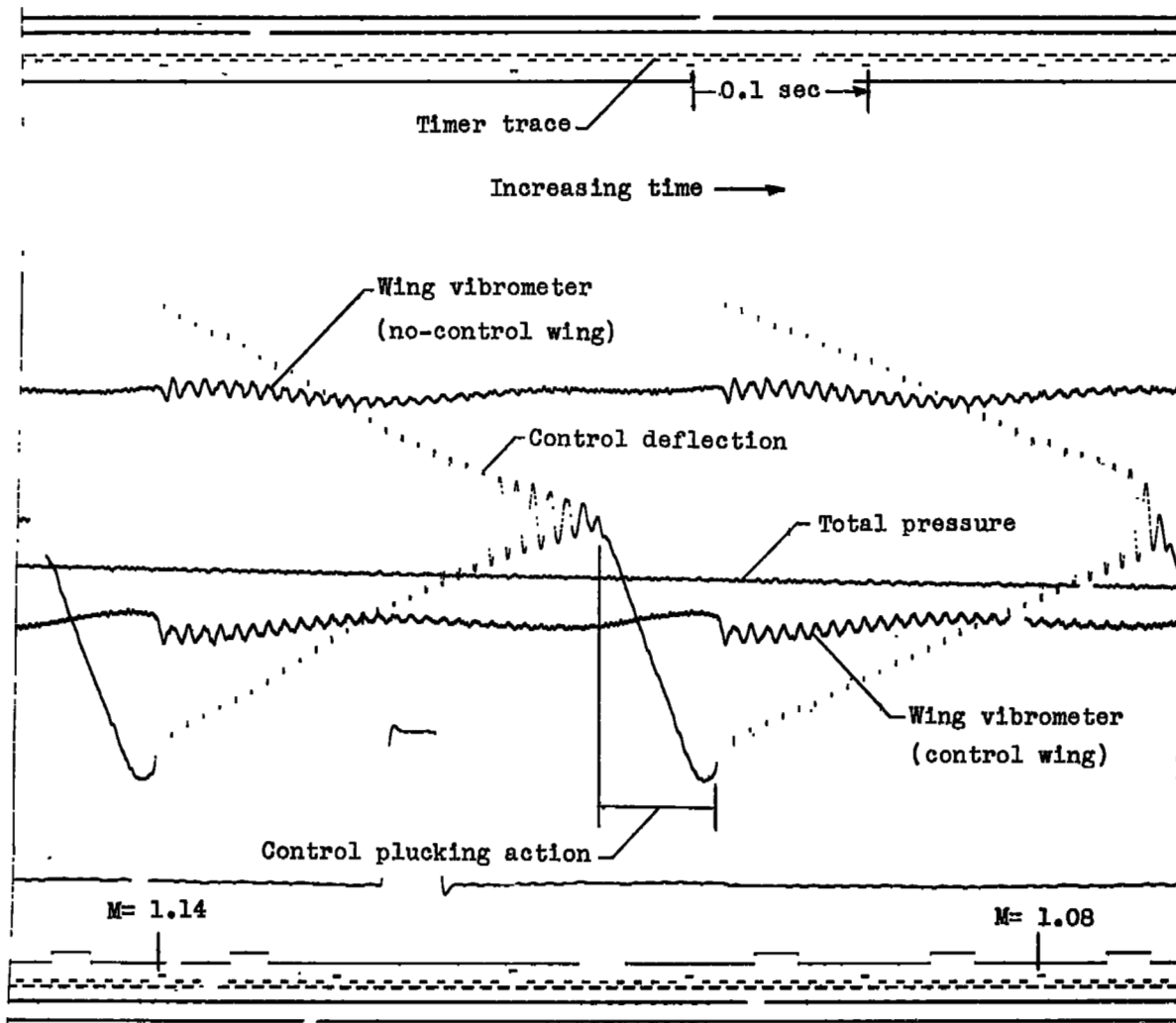


Figure 5.- Variation of dynamic pressure with Mach number.



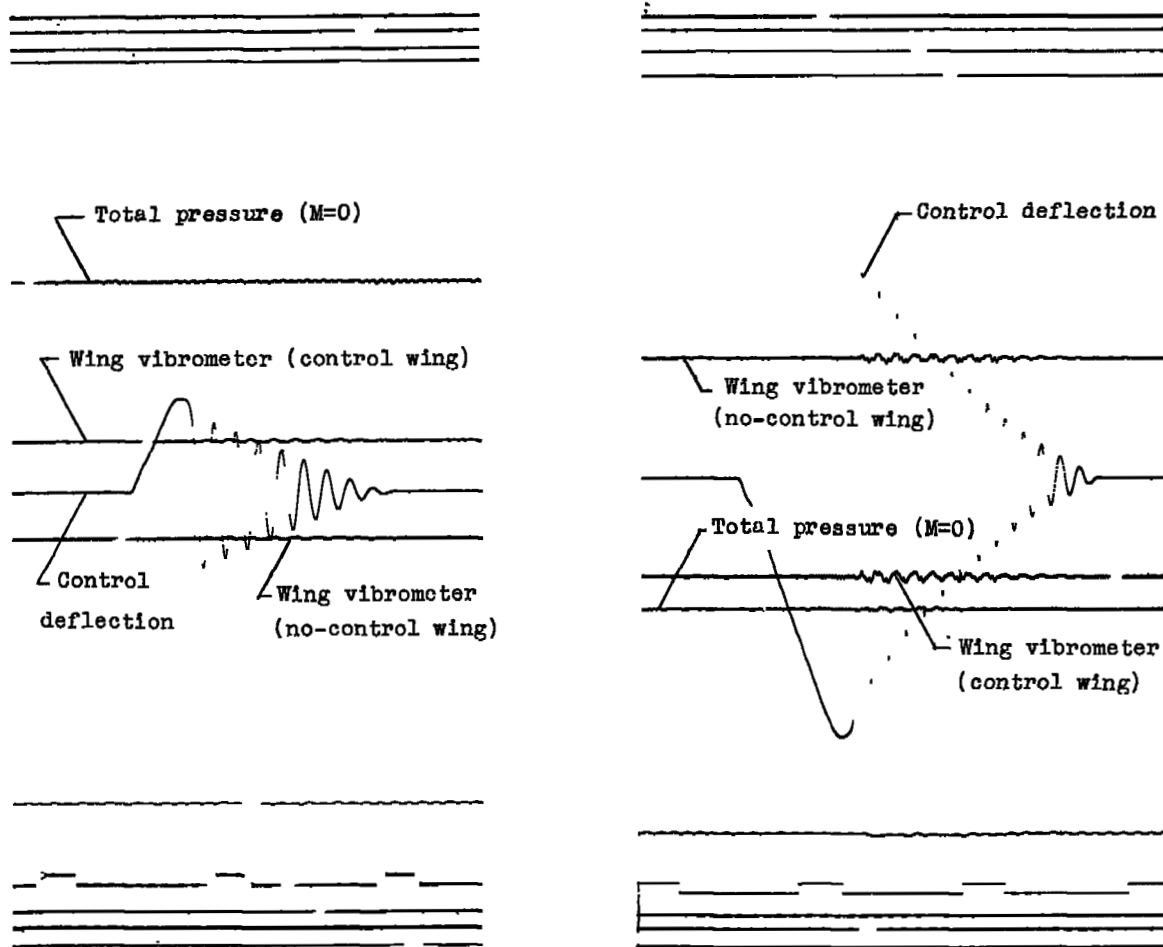
(a) Model A.

Figure 6.- Sample telemeter records.



(b) Model B.

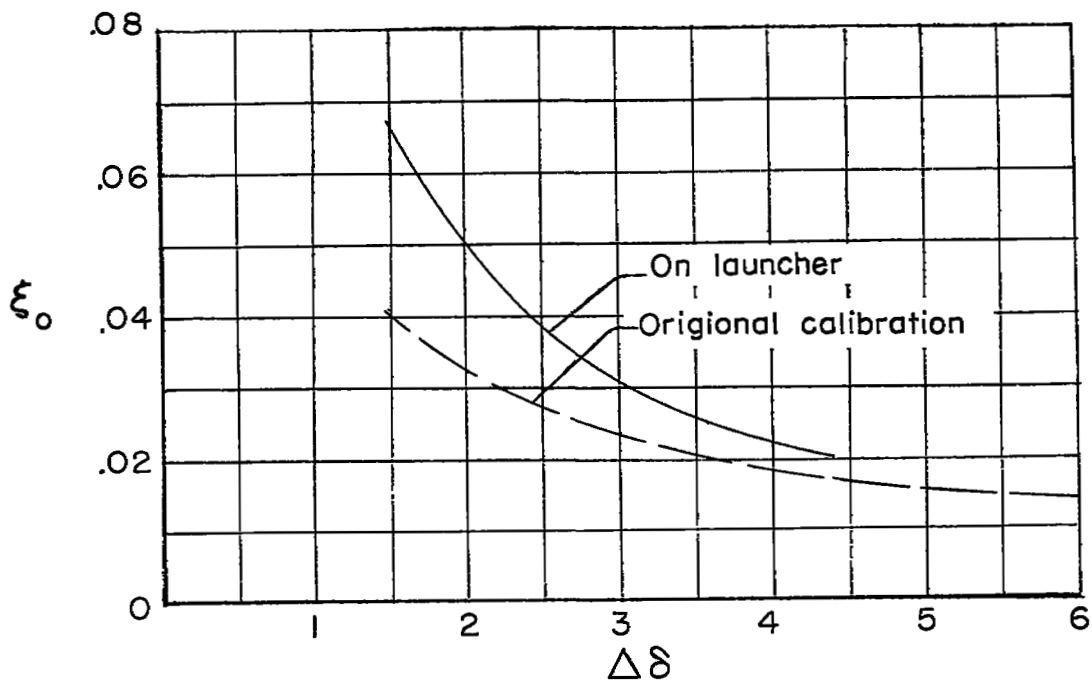
Figure 6.- Continued.



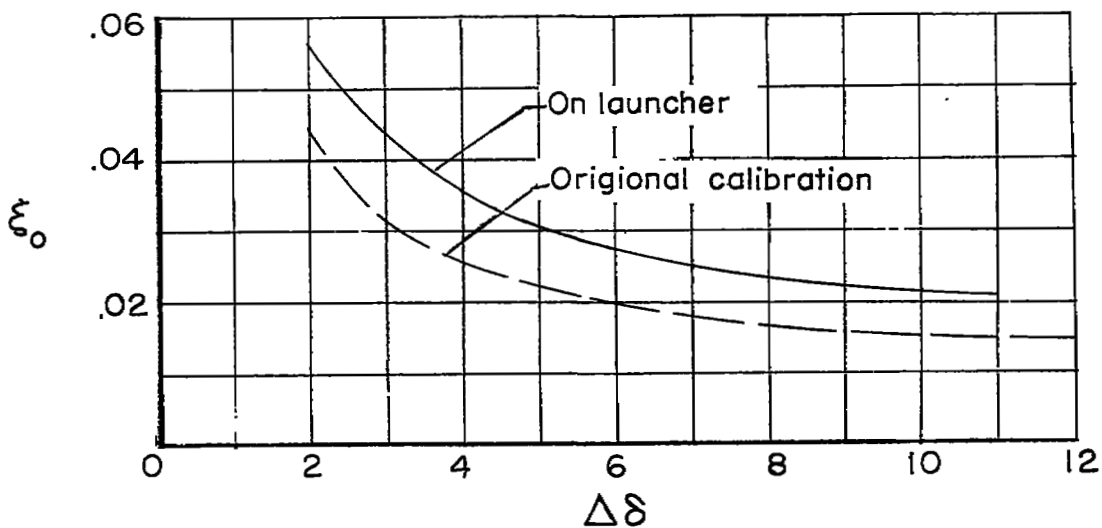
(c) Still-air control response to a step input (on launcher). Model A.

(d) Still-air control response to a step input (on launcher). Model B.

Figure 6.- Concluded.



(a) Model A.



(b) Model B.

Figure 7.- Variation of measured tare damping with oscillation amplitude.

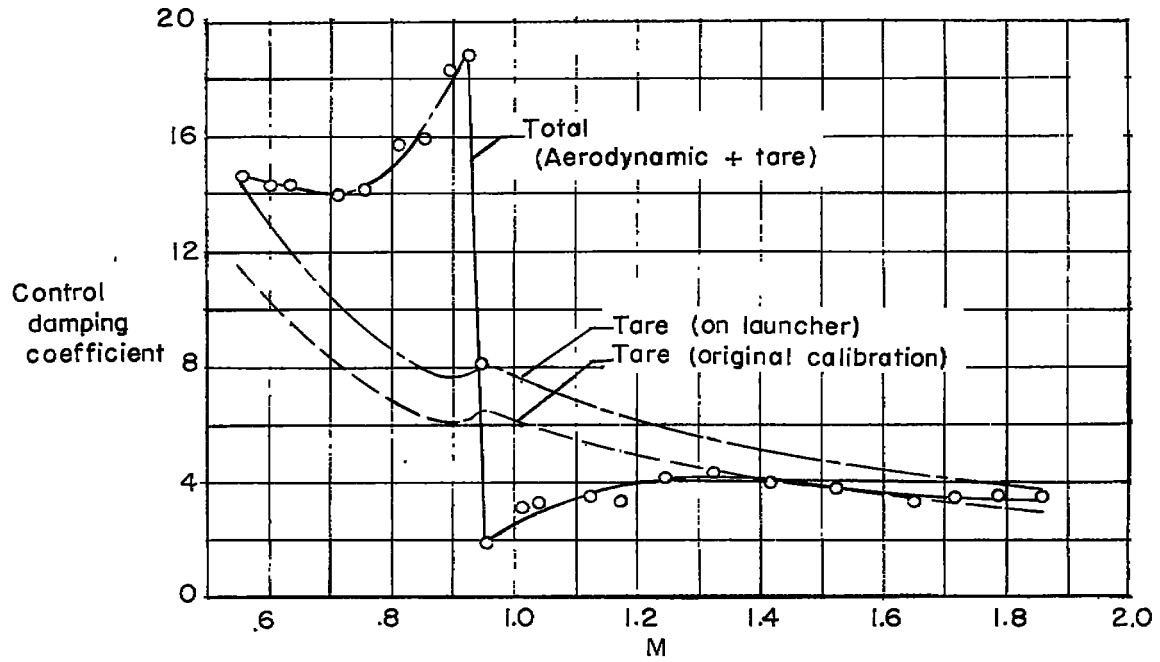
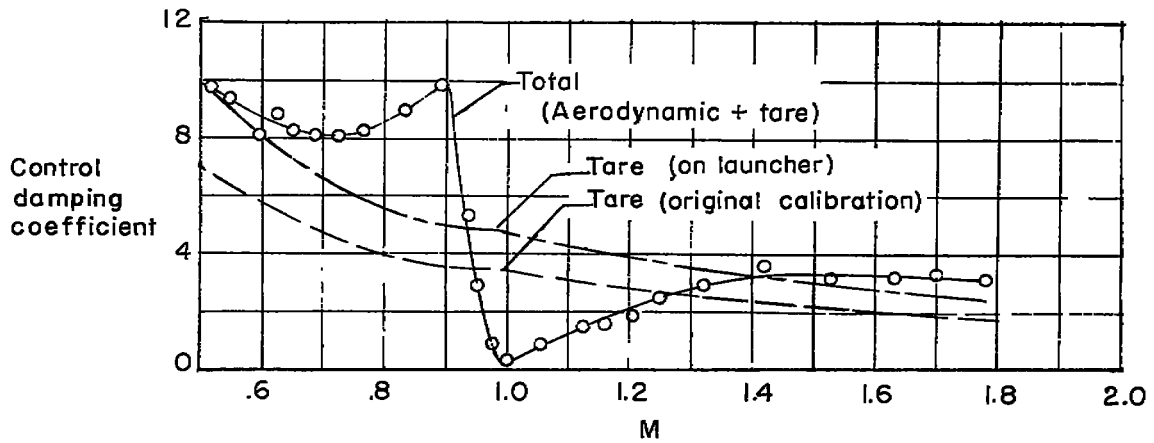
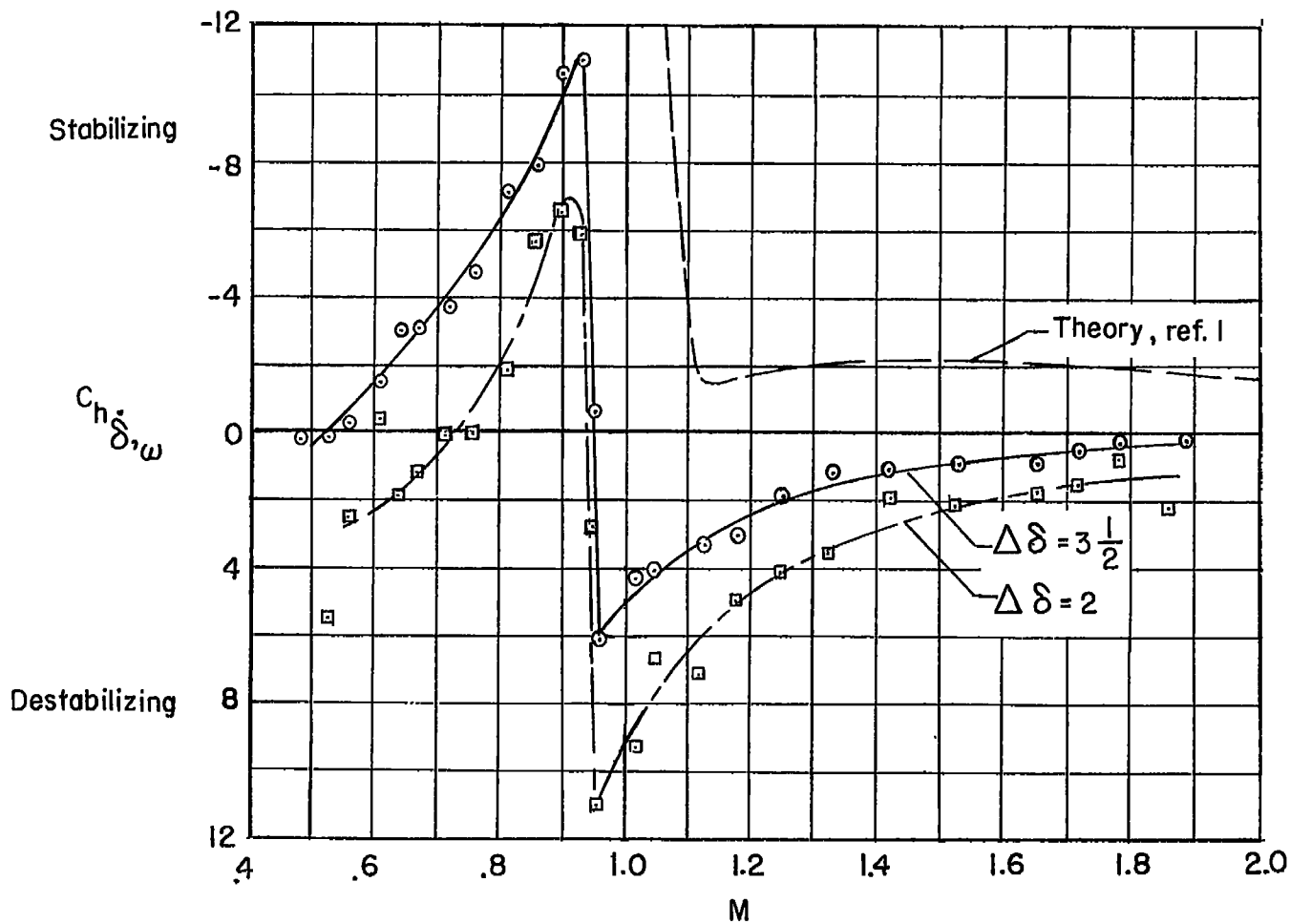
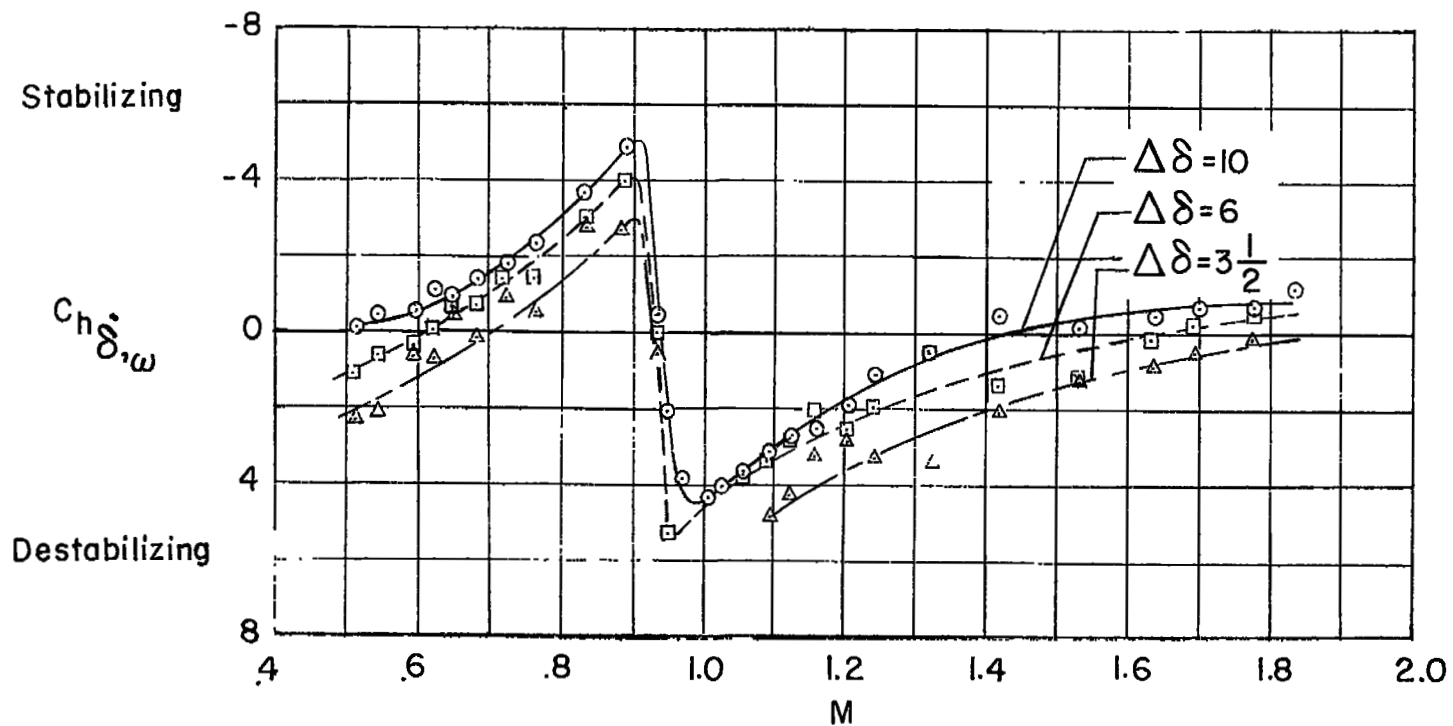
(a) Model A; $\Delta\delta = 3.5^\circ$.(b) Model B; $\Delta\delta = 10^\circ$.

Figure 8.- Variation of control damping coefficient with Mach number.



(a) Model A.

Figure 9.- Variation of control damping coefficient with Mach number for various oscillation amplitudes.



(b) Model B.

Figure 9.- Concluded.

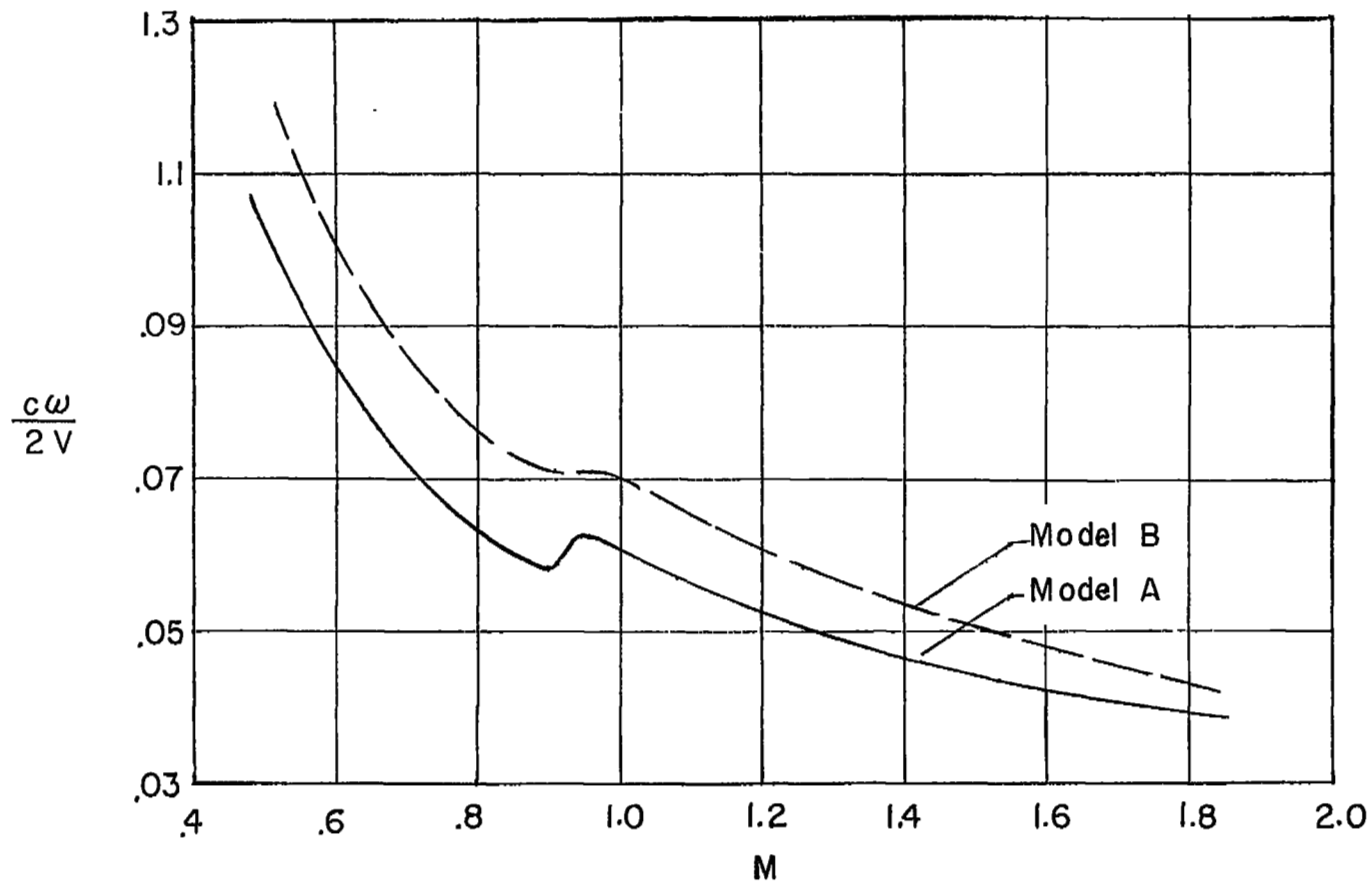


Figure 10.- Variation of reduced frequency parameter with Mach number.

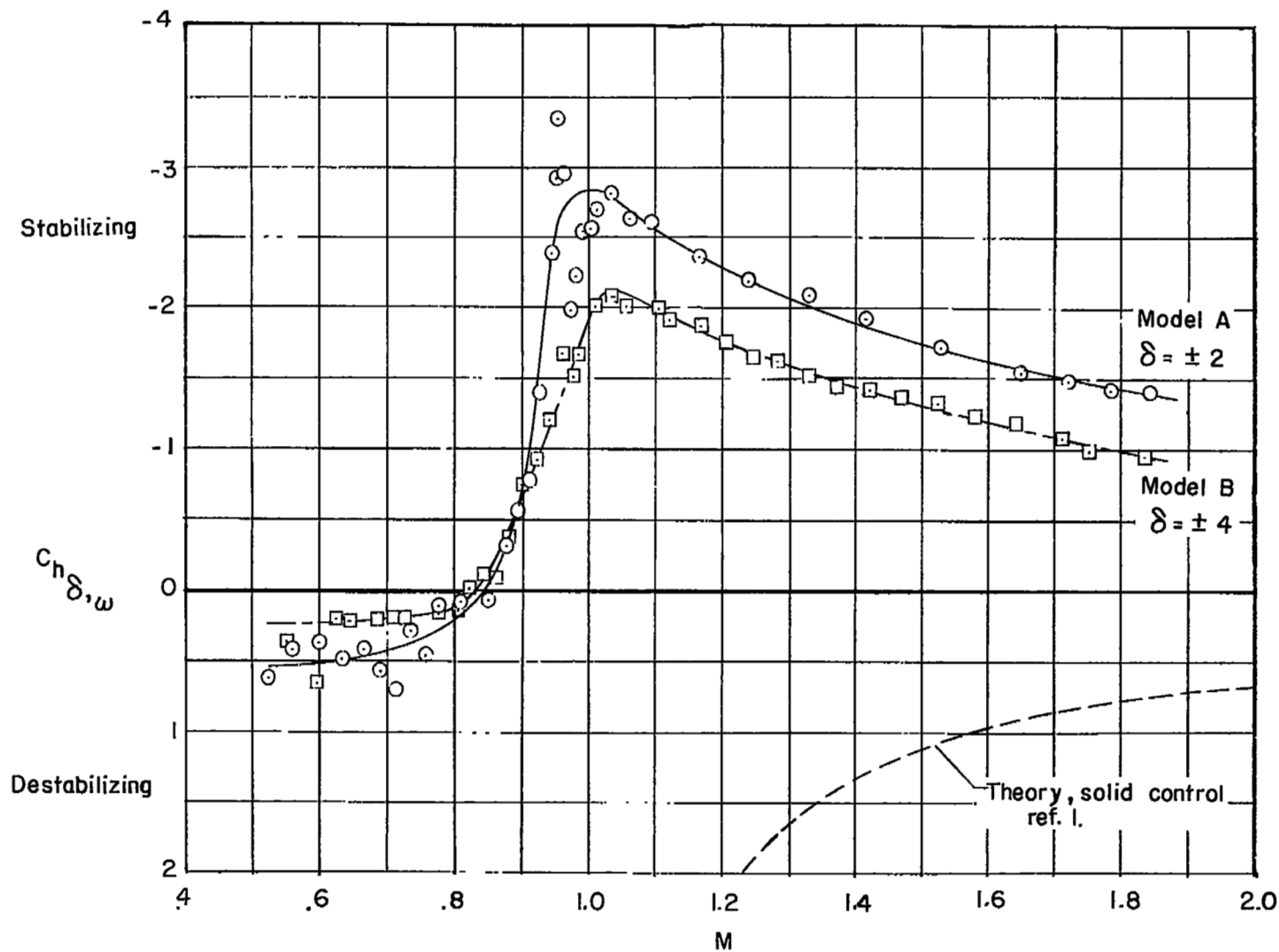


Figure 11.- Variation of control restoring-moment coefficient with Mach number.